CrossMark

RESEARCH PAPER

Novel prototyping method for microfluidic devices based on thermoplastic polyurethane microcapillary film

Zheyun Xu[1] · Feng Jiang[1] · Zhongbin Xu[1] · Haoyan Xu[2] · Xiaodong Ruan[3]

Abstract Thermoplastic polyurethane microcapillary film (TPU-MCF), as a novel extruded product, inherently contains an array of circular micron-sized capillaries embedded inside the polymer matrix. With the aid of simple laser cutting and conventional sealing technologies, a rapid prototyping method for microfluidic devices is proposed based on the ready-made microstructure of MCFs. Two functionalized microfluidic devices: serpentine micromixer and multi-droplet generator, are rapidly fabricated to demonstrate the advantages and potential of employing this new method. The whole proof-of-concept fabrication process can be completed in 8–10 min in a simple way; each procedure is repeatable with stable performance control of microfluidic devices; and the material cost can be as low as $0.01 for each device. The TPU-MCF and this novel method are expected to provide a new perspective and alternative in microfluidic community with particular requirements.

✉ Zhongbin Xu
xuzhongbin@zju.edu.cn

✉ Xiaodong Ruan
xdruan@zju.edu.cn

1 Department of Chemical Engineering and Biochemical Engineering, Institute of Process Equipment, Zhejiang University, Hangzhou 310027, China

2 Faculty of Information Technology, Zhejiang University, 38 Zheda Road, Hangzhou 310027, China

3 The State Key Laboratory of Fluid Power Transmission and Control, Zhejiang University, 38 Zheda Street, Hangzhou 310027, China

1 Introduction

For nearly three and half decades since microfluidic device has first emerged in early 1980s, researchers have rapidly been building a large body of knowledge in this field. The functional components of all microfluidic systems are microchannels—conduits for fluids that enable the rational transport and mixing of reagents. Along with more and more diverse applications proposed by microfluidic researchers, the comprehensive understanding of optimal base materials for fabricating microfluidic devices gains momentum.

Now, most of the microfluidic devices are employing materials such as silicon (Gravesen et al. 1993), glass (Park et al. 2009), SU-8 (Martinez et al. 2007), cloth (Nilghaz et al. 2012), papers (Martinez et al. 2008; Ballerini et al. 2012) and polymers like PMMA (Zhang et al. 2009) and PDMS (Bruzewicz et al. 2008; Weibel et al. 2005; Jeon et al. 2000), which becomes rather popular thanks to soft lithography. However, there are still challenges for these fabrication technologies to be dominant because of their intrinsic disadvantages. Manufacturing process of polymer-based devices always involves generation of toxic residuals, imposing safety concern on users and objects of research (Regehr et al. 2009; Lee et al. 2003). Most microchannels fabricated by conventional technologies like hot embossing, imprinting and patterned paper are rectangle-like and flat, despite the fact that the improved soft lithography can easily form rounded channels on PDMS by reflowing positive photoresist, which are mainly employed in fabricating micropumps and valves though (Unger et al. 2000; Fordyce

🖄 Springer

et al. 2012). Besides, for conventional base materials like polymer and glass, microchannels built at the very beginning are completely open, that is, every corner and edge of the whole flow path should be carefully sealed subsequently, which demands a strict requirement on the sealing effect. Also, once assembled completely, it is normally hard to stretch or bend the bulk device to a great extent in 3D, as the large shape change may severely deteriorate microfluidic function and damage the device, despite the fact that some researchers had tried uniaxial and planar stretch on PDMS device to culture cells (Shao et al. 2013; Carpi and Piel 2014). From the perspective of design, the traditional fabrication process of microfluidic device can be conceptualized as "zero to one"; fabrication starts with a zero basis without any ready-made structure; and each functional microchannel conduit needs to be built from the very beginning, which hinders the product repetitiveness and batch production.

As this field keeps maturing, the demand for alternative materials with unique properties, even ready-made microstructure, for speeding fabrication process of microfluidic devices has naturally increased (Kim et al. 2010; Wu et al. 2013). Microcapillary films (MCFs) are a class of novel, extrusion-processed, polymer material containing an array of continuous and parallel capillaries that run along the film's length (Hallmark et al. 2005). MCFs can be considered as hybrid between hollow fiber, plastic film and closed-cell polymer foam by virtue of the product's external film-like geometry, the structure of capillaries inside the polymer matrix and the anisotropic nature of the void age within the product. In recent years, the employment of MCFs extruded with different polymers in microfluidics has boomed. Hornung et al. firstly explored the hydrodynamic response and heat transfer performance of polyolefin MCFs along with proof-of-concept invention using MCFs as chemical microreactors (Hornung et al. 2006; Hallmark et al. 2008). Hallmark et al. (2009) established a successful method for microslugs or microdrops emulsion based on a polyolefin plastomer MCF, in whose research the continuous phase flow directly ran within the capillary, while the disperse phase was imported by inserting a hypodermic needle into the capillary through the side of MCF. Darton et al. (2011) showed that the surface-functionalized microcapillary films extruded with ethylene–vinyl alcohol copolymer (EVOH) can be used as a disposable absorbent material for fast cation-exchange separation of proteins. Also, some researchers turned their attention on the MCFs made with fluorinated ethylene propylene (FEP). Elvira et al. (2013) employed FEP MCFs as flow reactor systems for the singlet oxygen-mediated synthesis of ascaridole. Reis and Puma (2015) also demonstrated the fluoropolymer microcapillary film as a new, flexible and inexpensive platform for rapid photochemical transformations, high-throughput

process analytics and photochemical synthesis. In miniaturized point-of-care testing and field diagnostic applications, Edwards et al. (2011) presented a simple device for multiplex quantitative enzyme-linked immunosorbent assay (ELISA) made from FEP MCFs. Castanheira et al. (2015) invented a rapid, low-cost, sensitive and precise FEP MCFs microfluidic platform for multiple cytokine detection and quantitation. Integrated with a smartphone, the fluoropolymer MCF was adopted as a power-free detection system named MCF phone for portable colorimetric and fluorescence quantitative sandwich immunoassay detection of prostate-specific antigen (PSA) by Barbosa et al. (2015). In all previous researches, the structure of MCFs is almost intact, and no connection exists among the capillaries.

In this technical note, the MCFs are extruded with high-performance extrusion-grade thermoplastic polyurethane, which offers good mechanical properties and ultraviolet stability. The film in this study contains an array of micronsized rounded capillaries fabricated in one-stage formation. Combining with laser cutting technology and conventional sealing technology, a new method for rapidly prototyping the microfluidic system is presented. In this novel prototyping process, functional microfluidic sections are directly cut out by laser on the MCFs along the thickness direction, distinguished from the previous MCFs application researches, which maintained the structural integrity of MCFs; then, the cutting zone and designated capillaries of MCFs are selectively sealed by conventional materials to form a integral sealing. The capillary structure within the polymer matrix largely shortens the time necessary for fabricating microchannels from zero like soft lithography; in this way, reasonable pattern design plus simple post-processing can quickly accomplish a completed microfluidic product. Namely, the MCFs can be used as a semifinished microfluidic product; thus, the fabrication process turns to "half to one"—an advanced design concept compared to traditional "zero to one." To demonstrate the advantages of utilizing TPU-MCF and this novel fabricating method in microfluidics, a serpentine micromixer and a multi-droplet generator were made successively by using only a short length of film, and positive results were achieved successfully.

2 Experimental

2.1 Preparation of TPU-MCF

In previous work, MCFs have been manufactured with a range of thermoplastic polymers by mature extrusion technology. In this study, the thermoplastic polyurethane (Tecoflex EG-85A, Lubrizol Corp, OH, USA) was used as raw material to produce MCF as shown in Fig. 1a. Relevant characterizations of thermoplastic polyurethane (TPU)

Fig. 1 **a** Extrusion process of TPU-MCF, **b** TPU-MCF sample, **c** view of cross section of TPU-MCF under optical microscope, and it contains 13 capillaries in total
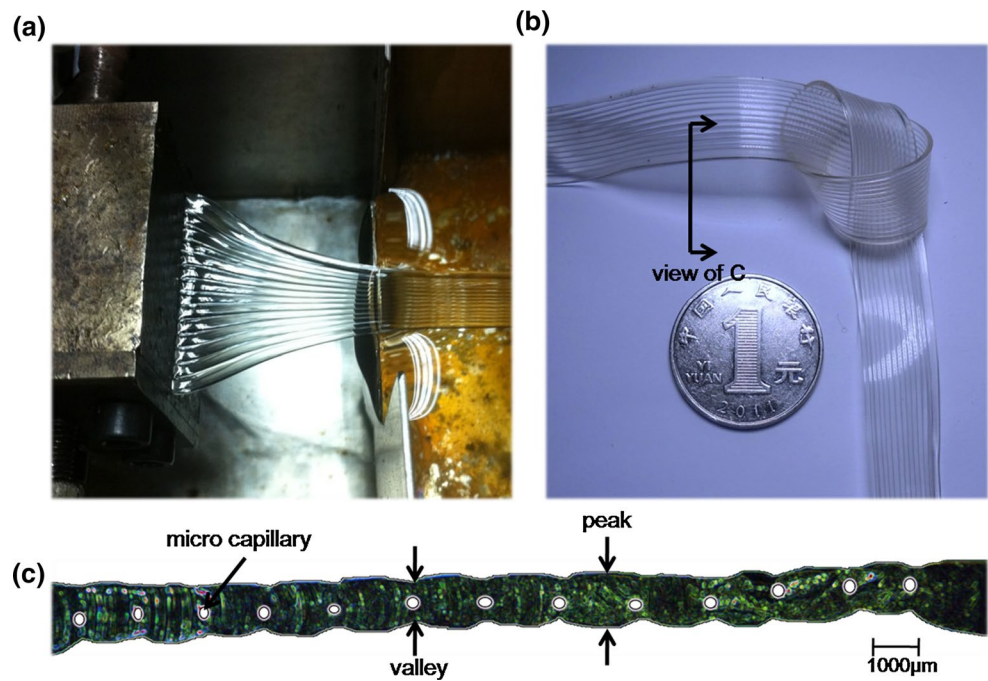

used and extrusion process are detailed in Online Resource 1. In principle, by tuning process parameters and adjusting die design, MCFs with desired cross-sectional size and certain number of capillaries can be easily obtained in one single process. At present, the MCFs with different capillary sizes can be steadily manufactured already in laboratory. The average hydraulic diameter of capillary is about 50–300 μm. All MCFs chosen for fabricating different devices in this technical note are uniform in size comprehensively. Thirteen capillaries are embedded inside MCFs as shown in Fig. 1c, and the average hydraulic diameter of capillary is 166 ± 15 μm, the average width of film is 14.7 mm, the average valley value of thickness is 620 ± 10 μm while the average peak value is 815 ± 10 μm as the surface geometry of TPU-MCFs is wave-like.

2.2 Fabrication of device

Combined with laser cutting technology and simple sealing materials, TPU-MCF-based microfluidic devices were conveniently and readily fabricated. A TPU-MCF serpentine micromixer was taken as an example to show the simple fabrication process step by step in Fig. 2. After cutting pattern was customized and loaded onto software (Corel DRAW X7®, Corel Corp, Ottawa, Canada), which runs over the laser cutter (Speedy 100R™, Trotec Corp, Wels, Austria), the machine automatically cut the desired pattern out (Fig. 2b). The working principle of laser cutting is to gasify polymer with instantaneous super-high energy, so the cutting process should be explored in advance to avoid excessive and insufficient gasification. By setting

the cutting power level and speed in controlling system, the depth cut could be precisely controlled. As plotted in Fig. 3, the cutting depth increased with the cutting speed decreasing from 10 to 1 (unit: cm/s), while the cutting power level was fixed at 80 (number means percentage of laser tube power, 45 W); partial penetration happened when the speed went to 2 and completely penetration happened when speed kept going down to 1. The cutting depth changed in similar way when the cutting power was altered with fixed cutting speed. Figure 3 also shows that the cutting power has a weaker impact than cutting speed on cutting depth comparatively. As a consequence, on the premise of getting desired cutting depth, the cutting speed was mainly controlled coupling with alternative cutting power to smaller the heat-affected zone on cutting edges for good cutting quality. Here, three rectangles were cut out: left bigger one, 1.5 mm × 2.5 mm (length × width), smaller one, 0.5 mm × 2.5 mm; and right one, 0.5 mm × 3.5 mm. The distance from left rectangle to right one was 5 cm. Then, appropriate capillaries were selected out for liquid flowing through, and the other capillaries in touch with the flow route were sealed by injecting liquid instant adhesive inside. The main effective component of instant adhesive is ethyl α-cyanoacrylate, which is well known as a kind of colorless, transparent and low-viscosity liquid quite suitable for bonding wood, rubber and plastic, etc. As only a very small amount of instant adhesive was injected inside to block the specific capillaries rather than filling up all the capillaries, the flexibility of MCFs is hardly changed. During the experiments, no breakage or deformation caused by instant adhesive was observed, while this adhesive did
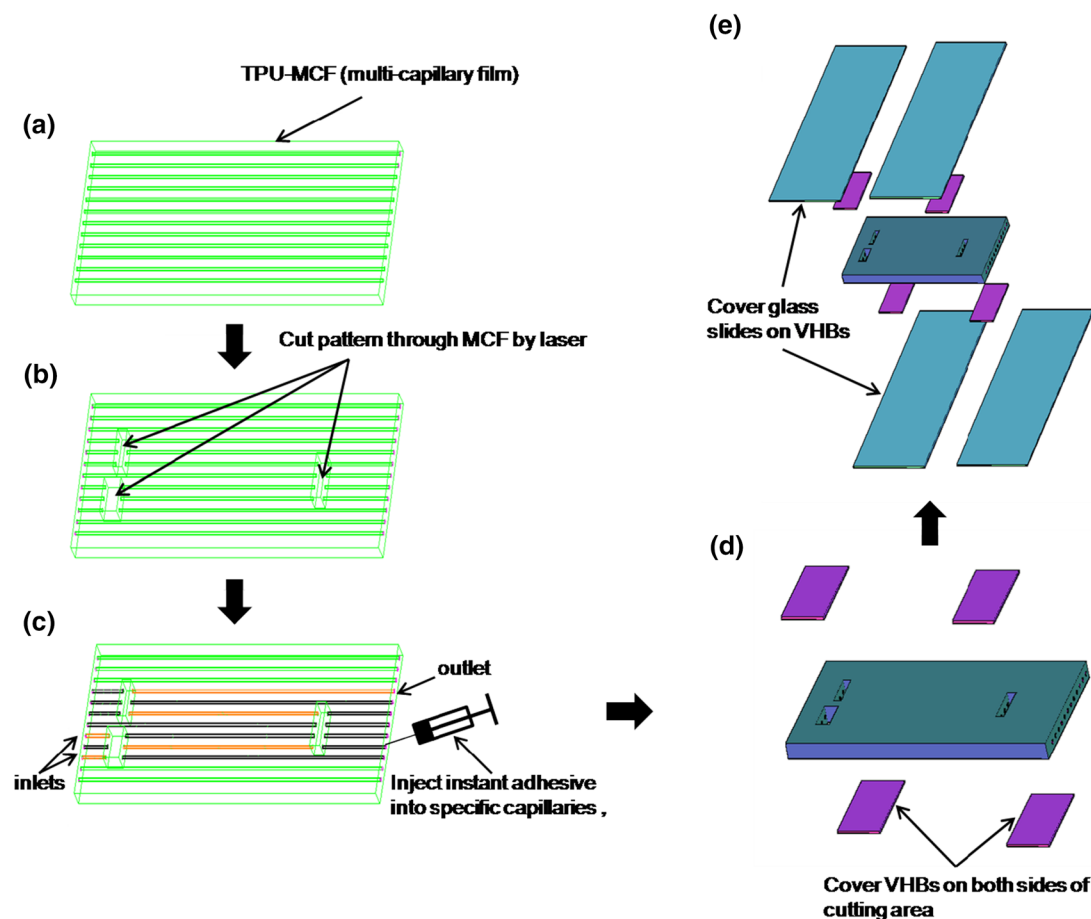
Fig. 2 Step-by-step schematic diagrams depicting the fabrication process of TPU-MCF serpentine micromixer. **a** A certain length of MCF, 10 cm in experiment; **b** cut designed pattern through the direction of thickness of MCF by laser cutting machine connected to computer control system. **c** Inject instant adhesive manually by syringe into some capillaries for sealing. *Black capillaries* were filled up, while *yellow ones* left clear for flows to run through. **d** Cover soft VHB adhesive tapes on *top* and *bottom* sides of cutting area for completely sealing. **e** Put glass slides on VHB tapes for observation and extra protection (color figure online)

affect the outside surface quality of MCFs when it solidified on outside surface. Designated capillaries can be easily reached using syringe with hollow steel needles (Φ200 μm). As shown in Fig. 2c, black capillaries were filled with adhesive, while yellow ones left untreated. Following the solidification of adhesive, two pieces of VHB tapes (VHB™4910 tape, 3 M Corp, Austin, TX, USA) were pasted on the top and bottom surfaces of cutting area (Fig. 2d). The wave-like surface of MCF is not easy to fit for conventional adhesive tape, but the polyacrylate VHB tapes solved this problem because of its excellent flexibility and malleability. It is worth noting that the sealing zone is restricted to the cutting area and specific capillaries rather than the whole flow path like conventional technologies, which lowers the risk of sealing failure. For a better protection and observation, glass slides were put on the surfaces of VHB tapes as shown in Fig. 2e, but the glasses are not necessary if the device is used with a shape-changed status

in space-/stress-critical environment. If people worry, the exposed VHB tapes are somewhat vulnerable and the glass slides limit the flexibility, and it is recommended to adopt some transparent and flexible polymer films like Mylar film of different thicknesses, which can be commercially purchased. The robust test of seal was conducted and detailed in supplementary information (Online Resource 2).

2.3 Device examples

1, 5 % red dye solution and 1 % blue dye solution were prepared by mixing colored food dye powders with DI water. In the example of droplet generator, dimethyl carbonate (D110625-500 ml, Aladdin Corp, Shanghai, China) was selected as the oil phase of inflow. All the inflows were motivated by injection pumps (SPLab01, Shenbeng Inc., Baoding, China) of which motion parameters could be manually adjusted. Then, soft rubber tubes with hollow
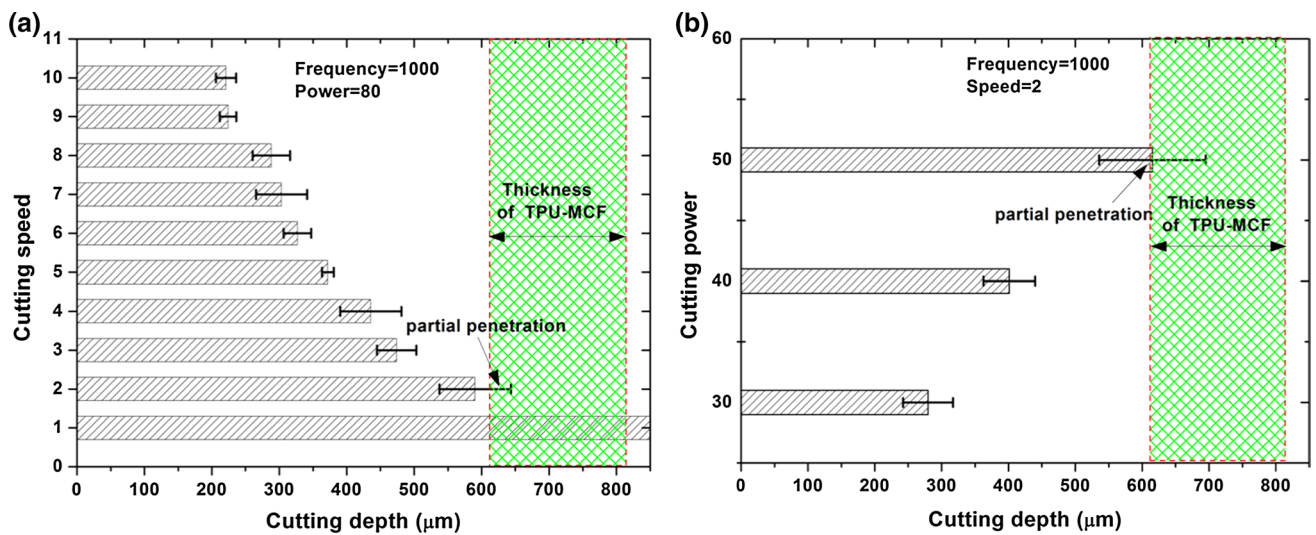
Fig. 3 **a** Change trend of cutting depth with cutting speed decreasing from 10 to 1 (unit: cm/s), while the power was fixed at 80; **b** the change trend of cutting depth with cutting power increasing from 30 to 50, while the cutting speed was fixed at 2. Laser tube total power: 45 W
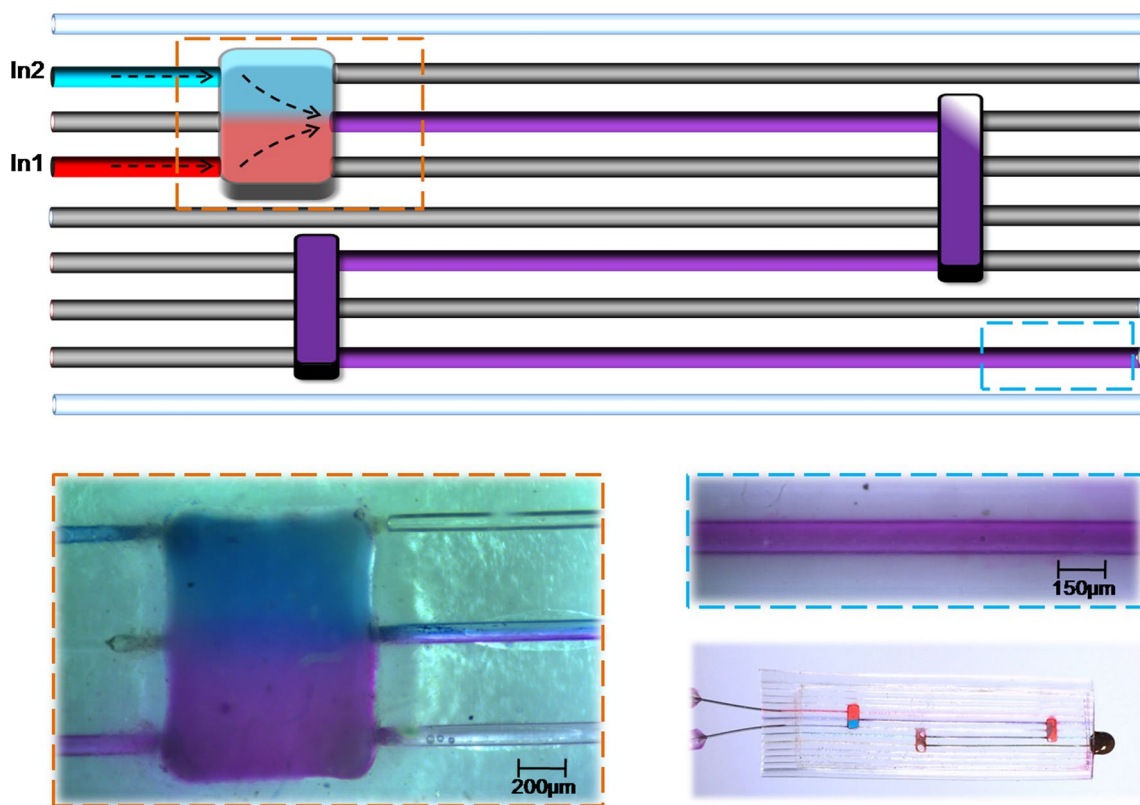
Fig. 4 Schematic picture of TPU-MCF serpentine micromixer with rectangle merging area. 1 % *red dye* solution (*In1*) and 1 % *blue dye* solution (*In2*) were pumped into MCF capillaries by injection pumps and forced to mix inside the *rectangle area*, and the initial combined flow of downstream presented obvious stratification shown in *orange dot line frame*, while the final outflow became uniform shown in *blue dot line frame*, and inflow rates here were set at 50 µl/m for both. Photograph of serpentine micromixer with different solutions pumped inside was exhibited at *bottom right corner* (color figure online)

steel needles (Φ200 μm) at end were used to connect pumps and TPU-MCF-based devices. The needles were directly plugged into corresponding capillaries in need (see Fig. s5 in Online Resource 1).

In the first example, a serpentine micromixer was designed and fabricated as schematically shown in top part of Fig. 4. Colored inflows were provided by two injection pumps connecting In1 and In2. 1 % red dye solution was injected into In1, while blue dye solution into In2. Colored solutions were forced to contact and run along the serpentine flowing route. Obvious stratification at initial downstream (bottom left corner of Fig. 4) and uniformity (bottom right corner of Fig. 4) at the final outlet was observed. Results were photographed by optical microscope (SMZ850T, OPLENIC Inc., Hangzhou, China). Both inflow rates here were set at 50 μl/m.

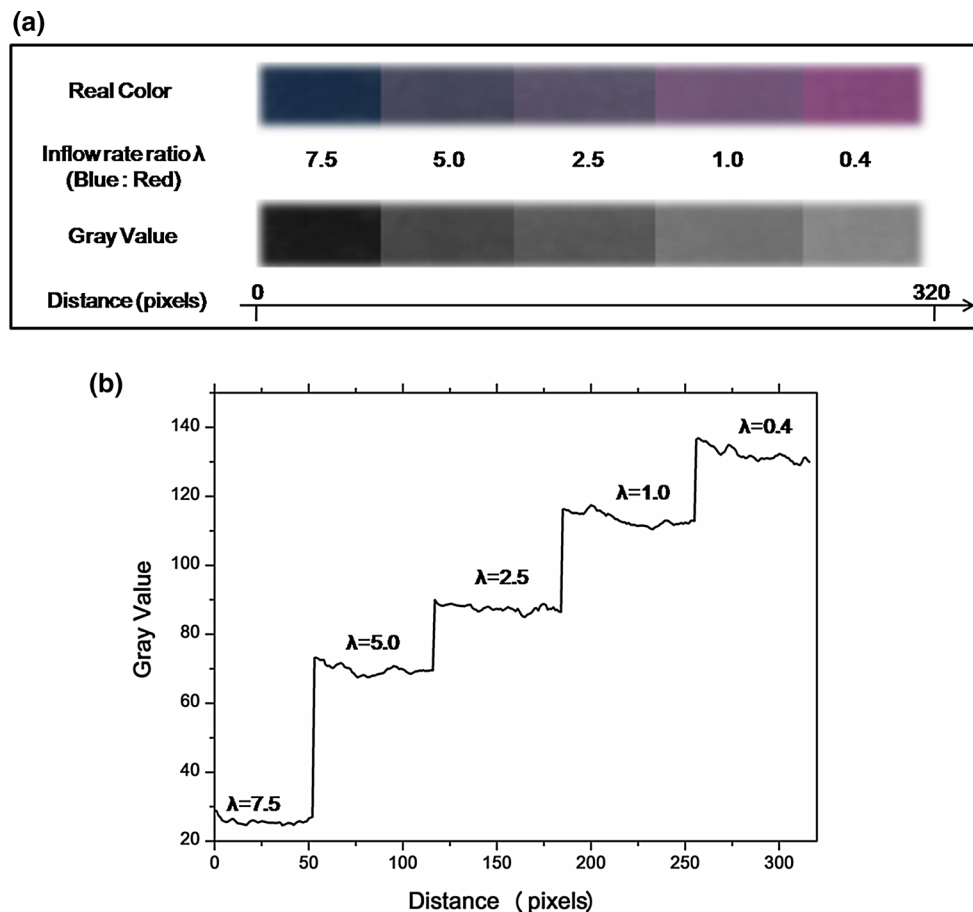As presented in Fig. 5, different combinations of inflow rates (blue/red(μl/m): 150/20, 100/20, 50/20, 20/20 and 20/50) were experimented, and the final outcomes were collected, respectively. Then, the variation of the colors of outcomes was analyzed and plotted into curves after transferring the colors to gray value by software (ImageJ, Open Source Software developed by NIH). The ratio of blue inflow rate to red one was defined as λ (7.5, 5.0, 2.5, 1.0 and 0.4 correspondingly here). Obviously, the gray value
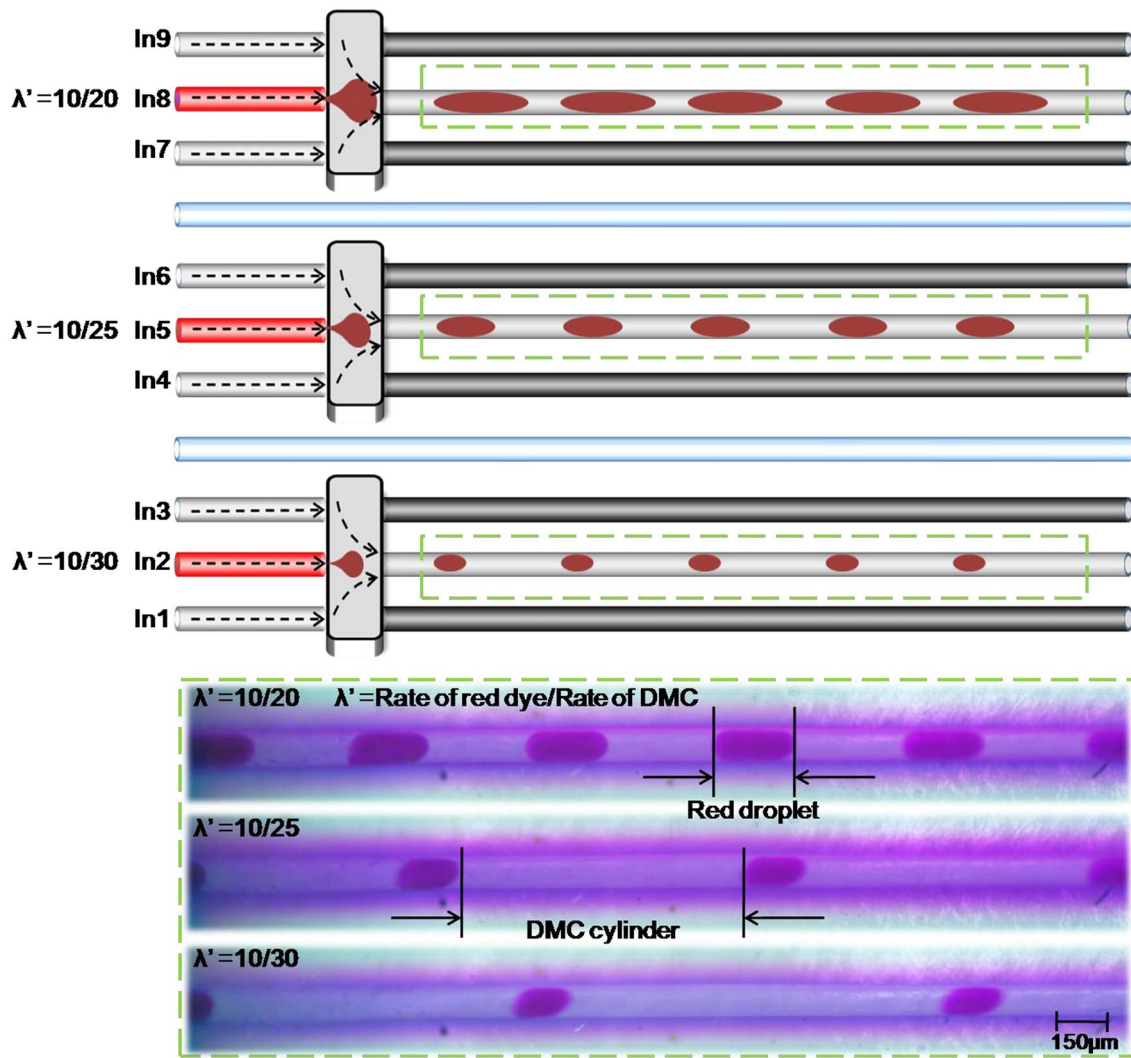
presented a step increase as λ went through a step decrease. This example demonstrates the capacity of this prototyping method for rapidly turning MCFs into a simple serpentine micromixer. Also, it is possible to mix more kinds of inflows at the same time by utilizing more capillaries of MCFs.

Through specific cutting pattern design, a multi-droplet generator based on TPU-MCF was attempted. Flow-focusing principle was adopted. Three 0.5 mm × 2.5 mm rectangles, each of which crossed three capillaries, were cut as shown in the top part of Fig. 6, which meant that three non-interfering droplet generating sections were produced on the same sample. Injection pumps injected 5 % red dye solution into In2,5,8 at a rate of 10 μl/m, dimethyl carbonate (DMC) into In1,3 at rate of 30 μl/m, DMC into In4,6 at rate of 25 μl/m and DMC into In7,9 at rate of 20 μl/m. It is notable that DMC inflow entrained red droplets in the downstream, and the distribution of red droplets varied due to the change of DMC inflow rates. The highest DMC inflow rate 30 μl/m led to the shortest length of red droplet and longest length of DMC cylinder.

Another set of droplet experiment was specially conducted for a further understanding on the principle of droplet generating. The ratio of red inflow rate to DMC inflow rate was defined as λ', and the ratio of red droplet

Fig. 5 Result of testing serpentine micromixer. **a** Inflow rates were set as: *In2/In1* (μl/m) = 150/20, 100/20, 50/20, 20/20 and 20/50. The final homogenous outflow showed *distinct colors* with varied relative proportions of inflows. These *colors* were also transferred into *gray value* for comparison; **b** the *gray value* went through a step growth as the proportion of *blue solution* steppedly decreased (color figure online)


(a)

Real Color					
Inflow rate ratio λ (Blue : Red)	7.5	5.0	2.5	1.0	0.4
Gray Value					
Distance (pixels)	0				320

(b)

Fig. 6 Example of TPU-MCF multi-droplet generator. Dimethyl carbonate (DMC) was pumped into *In1,3* at rate of 30 μl/m, into *In4,6* at rate of 25 μl/m and into *In7,9* at rate of 20 μl/m, while 5 % *red dye* solution was pumped into *In2,5,8* at rate of 10 μl/m. In the *bottom* of photograph, the length of *red droplet* gradually became shorter as the flow rate of DMC solution went up. And the DMC cylinder became longer and longer correspondingly (color figure online)

length to DMC cylinder length was defined as λ'' to investigate the influence of varied λ' on λ''. λ' was adjusted from 0 to 3.0, and the downstream was photographed by optical microscope as shown in supplementary information (Online Resource 1). Through intelligent calibration and measurement in ImageJ, a series of data was obtained and plotted into curves by software (Origin 8®, OriginLab Corp, MA, USA). Figure 7a reveals that the length of red droplet in capillary increased from 0.056 ± 0.012 mm to 0.656 ± 0.010 mm monotonously in accordance with a linear function $y = 0.227\lambda'$ (R-Square = 0.996, here 0.227 is a fitting constant), while the length of DMC cylinder presented opposite change trend from 0.445 ± 0.007 mm to 0.053 ± 0.009 mm. As shown in Fig. 7b, the relationship between λ' and λ'' was figured out in high accordance with the form of exponential function ($\lambda'' = 0.8(1 - e^{0.9\lambda'})$, R-Square = 0.999). Original numerical data and theoretical explanation of droplet generating were particularized in supplementary information (Online Resource 1). The result can be used as guidance for producing multi-droplets based on TPU-MCF. The high integrity of capillaries inside TPU-MCFs in this method brings possibility to generate droplets in a large scale simultaneously and real-time comparison by applying different inflow parameters in different capillaries.
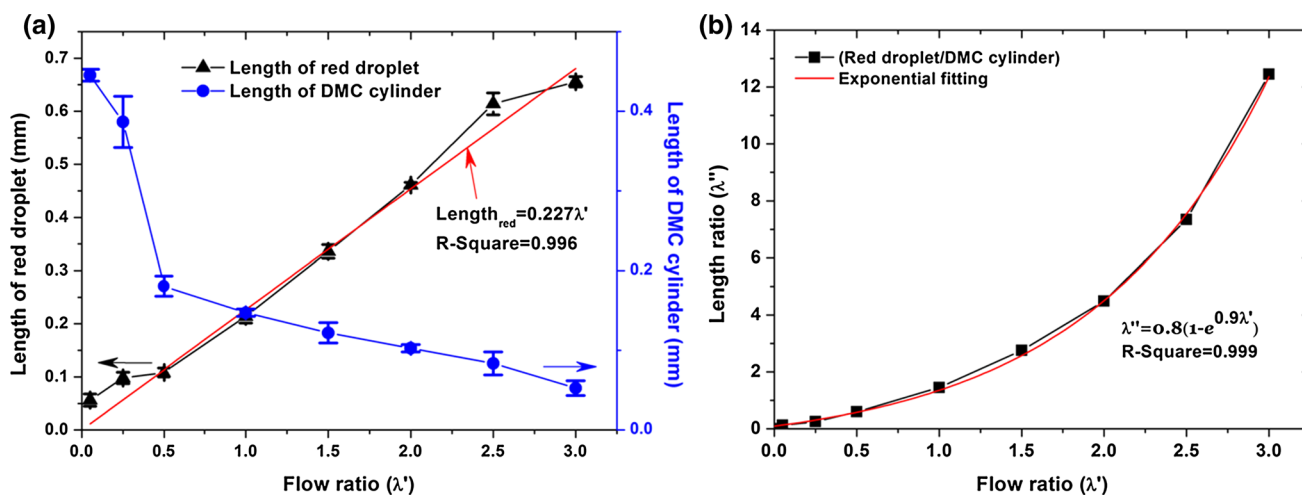
Fig. 7 Curves about the influence of inflow rates on droplet generating. **a** The inflow rate ratio λ' (red/DMC) was changed from 0 to 3.0, and the results were recorded. The length of red droplet in capillary increased from 0.056 ± 0.012 mm to 0.656 ± 0.010 mm in accordance with a linear fitting function $\text{Length}_{red} = 0.227\lambda'$ (R-Square = 0.996), while the length of DMC cylinder presented opposite change trend from 0.445 ± 0.007 mm to 0.053 ± 0.009 mm; exponential relationship ($\lambda'' = 0.8(1-e^{0.9\lambda'})$, R-Square = 0.999) between the length ratio λ'' (red/DMC) and λ' was plotted in **b**; the length ratio λ'' increases dramatically with λ' going up from 0 to 3.0 in experiments

3 Discussion

The proposed prototyping method based on TPU-MCFs has numbers of features compared with conventional fabrication technology. Clearly, extrusion process means that their unit cost could be similar to common plastic bags; thus, the eventual price depends on the types of polymer chosen. MCFs can be extruded from a range of thermoplastic polymers with tunable properties in a low-cost scalable procedure. Thermoplastic polyurethane used in this study was purchased at $9.00 per kg, so the material cost for microfluidic sample can be estimated at about $0.01 including the cost of the sealing materials. A possible merit of low cost is to create disposable systems, especially in biomedical applications to avoid contamination. In addition, the extrusion of MCFs is a continuous process, which means TPU-MCF-based microfluidic devices can be fabricated several orders of magnitude longer than other fabrication technologies, which might be suitable for applications requiring long-length microfluidic device. Besides, the whole proof-of-concept fabrication process of microfluidic devices with extruded MCFs only takes about 8–10 min: The laser cutting only costs about 1–2 min, and the most time-consuming part is the sealing procedure compared to other procedures relatively. However, considering specific microfluidic applications based on MCFs, only part of capillaries need to be sealed in fact. Taking a step back, even if all the capillaries (13 in total) are treated with instant adhesive, the time cost for sealing would be about 12 min for an experienced researcher. Besides, this process is of high freedom of manual operation and

position relevant in laboratory. But when it comes to mass production, this method will be somewhat labor intensive and impractical because of manual operation. Furthermore, this rapid prototyping method consisting of cutting and sealing technologies is highly controllable and repeatable. Researchers can be quickly skilled at this method after several attempts.

The nature of TPU-MCFs also enhances its potential capacity in microfluidics. Usually, the open-bottom rectangle channels in soft lithography and patterned paper are sealed by chemically bonding materials to a flat support substrate (*e.g.*, glass, silicon or PDMS), which limits the flexibility of devices. In contrast, Fig. 8 demonstrates that the bulk TPU-MCFs can be folded, twisted and spiraled to other rigid objective. And it is notable that even a complete 180° bending did not cause any capillary clogging. Moreover, rounded capillaries are embedded in the very middle place of TPU-MCF layer; thus, experimental components inside will be well protected by TPU walls from external disturbance. Besides, as described in the example of multi-droplet generator, the integrity of capillary offers another advantage, which could make it serve as a platform that allows different functionalized microfluidic sections to be put together on the same stripe of TPU-MCF. Currently, the possibility of coupling functional microfluidic sections together to constitute an integrated microfluidic system (*e.g.*, combining the multi-droplet generator with concentration gradient generator) is investigated. However, there also exist noteworthy shortcomings using TPU-MCF as microfluidic base material in some cases: The size of film cannot be adjusted once the MCF is extruded and cooled,
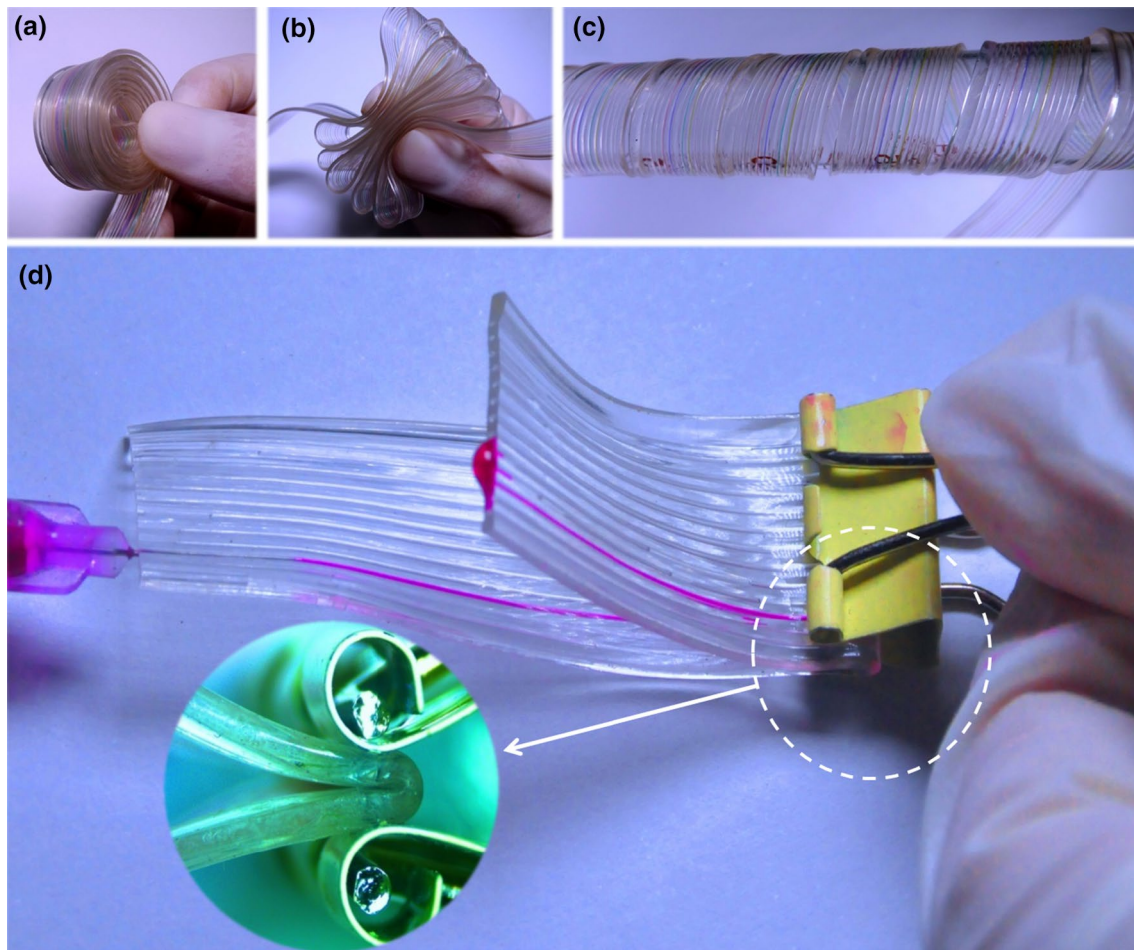
Fig. 8 Examples of shape changes on TPU-MCF. **a** A strip of TPU-MCF was spiraled into a small disk. **b** MCF was folded back and forth for 5 times. **c** MCF was entwined on a measuring cylinder. **d** A length of MCF was bended to a complete 180° turn with liquid flow in capillary unobstructed

and the diameter of all capillary is not uniform along the width direction, which may be inadequate for some highly accurate application.

4 Conclusion

In conclusion, the fusion of conventional technologies including laser cutting, extrusion and sealing contribute to a straightforward method to rapidly manufacture a family of microfluidic devices using thermoplastic polyurethane microcapillary film as the structural material. Based on ready-made TPU-MCFs, the whole "half to one" fabrication process from design concept to working device can be shortened and achieved in minutes. The simplification of fabrication enhances the repeatability of microfluidic devices without sacrificing the performance. It is further anticipated that the TPU-MCF could expand the repertoire of materials available in microfluidics and be considered as a practical alternative material in microfluidic field for laboratorial and industrial use.

Compliance with ethical standards

Conflict of interest The authors declare that they have no conflict of interest.

References

Ballerini DR, Li X, Shen W (2012) Patterned paper and alternative materials as substrates for low-cost microfluidic diagnostics. Microfluid Nanofluid 13(5):769–787

Barbosa AI, Gehlot P, Sidapra K, Edwards AD, Reis NM (2015) Portable smartphone quantitation of prostate specific antigen (PSA)

in a fluoropolymer microfluidic device. Biosens Bioelectron 70:5–14

Bruzewicz DA, Reches M, Whitesides GM (2008) Low-cost printing of poly (dimethylsiloxane) barriers to define microchannels in paper. Anal Chem 80(9):3387–3392

Carpi N, Piel M (2014) Stretching micropatterned cells on a PDMS membrane. J Vis Exp (83):51193. doi:10.3791/51193

Castanheira AP, Barbosa AI, Edwards AD, Reis NM (2015) Multiplexed femtomolar quantitation of human cytokines in a fluoropolymer microcapillary film. Analyst 140(16):5609–5618

Darton NJ, Reis NM, Mackley MR, Slater NK (2011) Fast cation-exchange separation of proteins in a plastic microcapillary disc. J Chromatogr A 1218(10):1409–1415

Edwards AD, Reis NM, Slater NK, Mackley MR (2011) A simple device for multiplex ELISA made from melt-extruded plastic microcapillary film. Lab Chip 11(24):4267–4273

Elvira KS, Wootton RC, Reis NM, Mackley MR, DeMello AJ (2013) Through-wall mass transport as a modality for safe generation of singlet oxygen in continuous flows. ACS Sustain Chem Eng 1(2):209–213

Fordyce PM, Diaz-Botia CA, DeRisi JL, Gomez-Sjoberg R (2012) Systematic characterization of feature dimensions and closing pressures for microfluidic valves produced via photoresist reflow. Lab Chip 12(21):4287–4295

Gravesen P, Branebjerg J, Jensen OS (1993) Microfluidics-a review. J Micromech Microeng 3(4):168

Hallmark B, Gadala-Maria F, Mackley MR (2005) The melt processing of polymer microcapillary film (MCF). J Non-Newton Fluid Mech 128(2):83–98

Hallmark B, Hornung CH, Broady D, Price-Kuehne C, Mackley MR (2008) The application of plastic microcapillary films for fast transient micro-heat exchange. Int J Heat Mass Transf 51(21):5344–5358

Hallmark B, Parmar C, Walker D, Hornung CH, Mackley MR, Davidson JF (2009) The experimental observation and modelling of microdroplet formation within a plastic microcapillary array. Chem Eng Sci 64(22):4758–4764

Hornung CH, Hallmark B, Hesketh RP, Mackley MR (2006) The fluid flow and heat transfer performance of thermoplastic microcapillary films. J Micromech Microeng 16(2):434

Jeon NL, Dertinger SK, Chiu DT, Choi IS, Stroock AD, Whitesides GM (2000) Generation of solution and surface gradients using microfluidic systems. Langmuir 16(22):8311–8316

Kim S, Kim HJ, Jeon NL (2010) Biological applications of microfluidic gradient devices. Integr Biol 2(11–12):584–603

Lee JN, Park C, Whitesides GM (2003) Solvent compatibility of poly (dimethylsiloxane)-based microfluidic devices. Anal Chem 75(23):6544–6554

Martinez AW, Phillips ST, Butte MJ, Whitesides GM (2007) Patterned paper as a platform for inexpensive, low-volume, portable bioassays. Angew Chem Int Ed 46(8):1318–1320

Martinez AW, Phillips ST, Whitesides GM (2008) Three-dimensional microfluidic devices fabricated in layered paper and tape. Proc Natl Acad Sci 105(50):19606–19611

Nilghaz A, Wicaksono DH, Gustiono D, Majid FAA, Supriyanto E, Kadir MRA (2012) Flexible microfluidic cloth-based analytical devices using a low-cost wax patterning technique. Lab Chip 12(1):209–218

Park JM, Evans AT, Rasmussen K, Brosten TR, Nellis GF, Klein SA, Gianchandani YB (2009) A microvalve with integrated sensors and customizable normal state for low-temperature operation. J Microelectromech Syst 18(4):868–877

Regehr KJ, Domenech M, Koepsel JT, Carver KC, Ellison-Zelski SJ, Murphy WL, Beebe DJ (2009) Biological implications of polydimethylsiloxane-based microfluidic cell culture. Lab Chip 9(15):2132–2139

Reis NM, Puma GL (2015) A novel microfluidic approach for extremely fast and efficient photochemical transformations in fluoropolymer microcapillary films. Chem Commun 51(40):8414–8417

Shao Y, Tan X, Novitski R, Muqaddam M, List P, Williamson L, Liu AP (2013) Uniaxial cell stretching device for live-cell imaging of mechanosensitive cellular functions. Rev Sci Instrum 84(11):114304

Unger MA, Chou HP, Thorsen T, Scherer A, Quake SR (2000) Monolithic microfabricated valves and pumps by multilayer soft lithography. Science 288(5463):113–116

Weibel DB, Kruithof M, Potenta S, Sia SK, Lee A, Whitesides GM (2005) Torque-actuated valves for microfluidics. Anal Chem 77(15):4726–4733

Wu J, Wu X, Lin F (2013) Recent developments in microfluidics-based chemotaxis studies. Lab Chip 13(13):2484–2499

Zhang W, Lin S, Wang C, Hu J, Li C, Zhuang Z, Yang CJ (2009) PMMA/PDMS valves and pumps for disposable microfluidics. Lab Chip 9(21):3088–3094